

DOI:10.1002/ejic.201300809

# Rhodamine-Based Chromo-/Fluorogenic Dual Signalling Probe for Selective Recognition of Hg<sup>II</sup> with Potential Applications for INHIBIT Logic Devices and Cell-Imaging Studies

Tarun Mistri,<sup>[a]</sup> Rabiul Alam,<sup>[a]</sup> Malay Dolai,<sup>[a]</sup>  
Sushil Kumar Mandal,<sup>[b]</sup> Pratik Guha,<sup>[a]</sup>  
Anisur Rahman Khuda-Bukhsh,<sup>[b]</sup> and Mahammad Ali\*<sup>[a]</sup>

**Keywords:** Mercury / Sensors / Logic gates / Cell-imaging / Fluorescence

A new rhodamine-based dual signaling probe (**L**<sup>3</sup>) has been found to display quick responses through visible colorimetric changes as well as fluorogenic properties on selective 1:1 binding to Hg<sup>2+</sup>, as delineated by absorption and fluorescence titrations as well as by Job's method and ESI-MS<sup>+</sup> studies. The fluorescent probe **L**<sup>3</sup> displays a 252-fold fluorescence enhancement on binding to Hg<sup>2+</sup>. A Benesi–Hildebrand fit of the absorption titration data gives  $K_d = (32.01 \pm 0.74) \mu\text{M}$  and a 1:1 binding stoichiometry. Owing to

its solubility in mixed organic/aqueous solvents as well as its cell permeability, **L**<sup>3</sup> could be used for in vitro/in vivo cell imaging of Hg<sup>2+</sup> with no or negligible cytotoxicity. The detection limit of Hg<sup>2+</sup> was calculated by the 3 $\sigma$  method to be 9.28 ng L<sup>-1</sup>. Moreover, the fluorescence of the **L**<sup>3</sup>-Hg<sup>2+</sup> system was turned off and its red colour disappeared when KI was added. Thus, the "OFF–ON–OFF" fluorescence sensing behaviour of **L**<sup>3</sup> observed in the presence of Hg<sup>2+</sup> and I<sup>-</sup> may find applications in devices with logic gate functions.

## Introduction

In recent years, the field of chemosensing has expanded very rapidly due to its advantages of quick response, good selectivity and high sensitivity and finds wide applications in various measurement devices in the fields of life sciences, environmental science, medical diagnostics and toxicological analysis.<sup>[1]</sup> In particular, it is highly demanding for the selective sensing of heavy metal ions such as Hg<sup>2+</sup>, Pb<sup>2+</sup> and Cd<sup>2+</sup>.<sup>[2]</sup>

Mercury has significant industrial and agricultural uses although it is known to be one of the most toxic heavy metals. It is widespread in air, water and soil, generated by many processes such as oceanic and volcanic eruptions, coal burning, combustion of fossil fuels, gold mining and solid-waste incineration. Mercury ions show a high affinity for thiol groups in proteins and enzymes, leading to the malfunction of cells and consequently causing health problems in the brain, kidney and central nervous system. Its accumulation in the body can be responsible for the develop-

ment of a wide variety of diseases, such as prenatal brain damage, serious cognitive and motion disorders, and Minamata disease.<sup>[3]</sup> Owing to the concern over its deleterious effects in humans, new mercury detection methods have been developed that are cost effective, rapid, facile and applicable in the environmental and biological milieux.<sup>[4]</sup>

The most common analytical methods used for the detection and quantification of mercury ions include atomic absorption and emission spectroscopy,<sup>[5]</sup> inductively coupled plasma mass spectroscopy (ICP-MS),<sup>[6]</sup> inductively coupled plasma atomic emission spectrometry (ICP-AES)<sup>[7]</sup> and voltammetry.<sup>[8]</sup> However, most of these methods are either very costly or time-consuming and not suitable for performing assays. Thus, over the past decade more attention has been focused on the development of efficient fluorescent chemosensors for the detection of Hg<sup>2+</sup> ions for real-time monitoring of environmental, biological and industrial samples.<sup>[4,9,10]</sup>

The sensing chemistry of the Hg<sup>2+</sup> ion is quite interesting. It is known to be a fluorescence quencher mainly due to its high atomic number (*Z*) and large spin–orbit coupling ( $\zeta$ )<sup>[11]</sup> but, in general, any optical feedback that translates the metal-ion–receptor binding phenomenon into a fluorescence turn-on (fluorescence enhancement) response is preferred over the fluorescence turn-off (fluorescence quenching) response process because quenching is not as sensitive as enhancement and, moreover, fluorescence "turn-off"

[a] Department of Chemistry, Jadavpur University, Kolkata 700032, India  
E-mail: m\_ali2062@yahoo.com  
<http://www.jaduniv.edu.in/profile.php?uid=30>

[b] Department of Zoology, Kalyani University, Kalyani 741235, India

Supporting information for this article is available on the WWW under <http://dx.doi.org/10.1002/ejic.201300809>.

probes may produce false positive reports caused by other quenchers present in practical samples. Thus, any sensor molecule that shows a fluorescence turn-on response and can also be used for the colorimetric detection of  $\text{Hg}^{2+}$  in aqueous or mixed aqueous/organic solvent systems is important from the viewpoint of its potential applications as a staining or imaging reagent for biological applications.<sup>[12]</sup>

The rhodamine framework is an ideal model for the construction of OFF–ON fluorescent chemosensors due to its particular structural properties.<sup>[13]</sup> Its derivatives with the spiro-lactam structure are found to be non-fluorescent, whereas opening of the spiro-lactam ring gives rise to a strong fluorescence emission along with a drastic colour change visible to the naked eye. Moreover, the rhodamine fluorophore exhibits good photostability, a high extinction coefficient and a longer emission wavelength (>550 nm), which is often preferred to avoid background fluorescence (below 500 nm).<sup>[13,14]</sup> It is also known to be an excellent candidate as a fluorescent sensor that can detect  $\text{Hg}^{2+}$  ions below 2 ppb.<sup>[13d]</sup> Thus, it provides both in-field detection through optical colour change as well as the edge in imaging studies through its OFF–ON fluorescent property. Because of all the above-mentioned advantages, rhodamine-based fluorosensors have become an attractive choice for the design of receptors for the  $\text{Hg}^{2+}$  ion.

On the other hand, remarkable progress has been achieved in recent times in the development of molecular systems that are capable of performing logic operations and are attractive for the construction of molecular devices that are demanded by information technology.<sup>[15]</sup> Also, their integration into arithmetic systems has brought chemists closer to the realization of a molecular-scale calculator (moleculator).<sup>[15c]</sup> Logic systems consisting of chemically encoded information as input and a fluorescence signal as output have received considerable attention and functions such as AND, NAND, OR, NOR, XOR, XNOR and INHIBIT have been widely explored.<sup>[16]</sup> In all molecular logic gates, the molecule demonstrates “ON” or “OFF” switching of the fluorescence signal, which equates to an output “1” or “0”, respectively, in response to the addition “1” or no addition “0” of the input chemicals. Such devices operate in wireless mode and have the potential for computation on a molecular level that silicon-based devices cannot address. Hence, they have possible applications in the development of electronic and photonic devices.

Therefore there is a need to develop new synthetic strategies, usually employing a structurally well-developed receptor unit in the fluoro-ionophore system that provides a reversible colorimetric as well as a fluorescent turn-on response essential for investigating intracellular  $\text{Hg}^{2+}$  ions with no or negligible cytotoxicity. In particular, such fluorescent chemosensors can be used not only for the selective detection of  $\text{Hg}^{2+}$  as a representative of heavy metal ions in organic/aqueous solutions and cells, but also for integrating these heavy metal ions in chemical-driven molecular machines in future molecular computing.

We present herein a new type of easily synthesizable rhodamine-based chemosensor with potential  $\text{N}_2\text{O}_2$  donor

atoms for the selective and rapid recognition of toxic  $\text{Hg}^{2+}$  ions that exhibits reversible fluorescence enhancement along with a colour change visible to the naked eye through metal-induced opening of the spiro-lactam ring in the xanthene moiety in an organic/aqueous medium with potential for biological cell imaging.<sup>[17]</sup> Also, this study has revealed new potential applications in the development of new-generation molecular electronic devices, a molecular INHIBIT logic gate, in which  $\text{Hg}^{2+}$  and  $\text{I}^-$  are used as chemical inputs and the fluorescence signal as output.

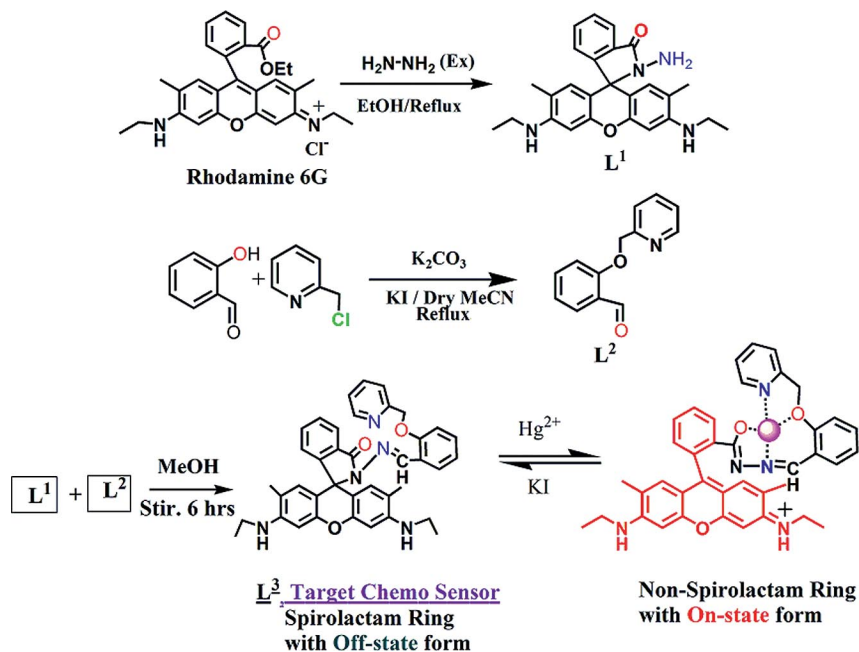
## Results and Discussion

Sensor  $\text{L}^3$  was easily synthesized by simple Schiff-base condensation between rhodamine 6G hydrazide ( $\text{L}^1$ ) and 2-(pyridin-2-ylmethoxy)benzaldehyde ( $\text{L}^2$ ) in methanol (Scheme 1) and thoroughly characterized by ESI-MS<sup>+</sup>,  $^1\text{H}$  and  $^{13}\text{C}$  NMR spectroscopy, and CHN elemental analysis. The structure of the probe was also analysed by single-crystal X-ray diffraction (see Table S1 in the Supporting Information) and the ORTEP view is shown in Figure 1. The characteristic peak at  $\delta = 64.79$  ppm in the  $^{13}\text{C}$  NMR spectrum corresponding to C4 in  $\text{L}^3$  suggests that it exists in solution predominantly in its colourless and fluorescence-inactive spiro-lactam form.<sup>[18]</sup> The crystal structure of  $\text{L}^3$  also clearly shows the unique formation of the spiro-lactam ring.

The spectrophotometric titration performed to analyse the interaction of  $\text{L}^3$  with  $\text{Hg}^{2+}$  at 25 °C in aqueous MeCN (4:6, v/v, HEPES buffer, pH 7.1) revealed that there is a gradual development of a new absorption band centred at around 529 nm on gradual addition of  $\text{Hg}^{2+}$  in the range 0–100.0  $\mu\text{M}$  (Figure 2, A) and it becomes saturated upon addition of around 1.20 equiv. of  $\text{Hg}^{2+}$  (Figure 2, B), the concentration of  $\text{L}^3$  being fixed at 20.0  $\mu\text{M}$ . A detectable change in the colour of the solution from colourless to orange-yellow (Figure 2, E) clearly demonstrated the formation of the ring-opened amide form of  $\text{L}^3$  upon binding to  $\text{Hg}^{2+}$ .<sup>[19]</sup> The composition and binding constant of the formed complex  $[\text{Hg}(\text{L}^3)]$  was determined by utilizing the Benesi–Hilderband equation (1)

$$\frac{(A_{\text{max}} - A_0)}{(A - A_0)} = 1 + \frac{1}{K[\text{Hg}^{2+}]^n} \quad (1)$$

in which  $A_0$  and  $A_{\text{max}}$  are the absorbances of the pure ligand in the absence of the metal ion and in the presence of excess metal ion, respectively. A plot of  $[(A_{\text{max}} - A_0)/(A - A_0)]$  vs.  $1/[\text{Hg}^{2+}]$  (Figure 2, C) gives a straight line with  $K_{\text{d}} = (32.1 \pm 0.74) \mu\text{M}$ . It also indicates a 1:1 ( $n = 1$ ) complexation between  $\text{L}^3$  and  $\text{Hg}^{2+}$ . The composition of the complex was also determined by Job's method (Figure 2D) and is supported by mass spectrometric analysis ( $m/z = 849.29$   $[\text{Hg}(\text{L}^3)(\text{H}_2\text{O})\text{Li}]^+$ ; see Figure S1 in the Supporting Information).



Scheme 1. Synthetic routes to chemosensor L<sup>3</sup> and its binding mode towards Hg<sup>2+</sup>.

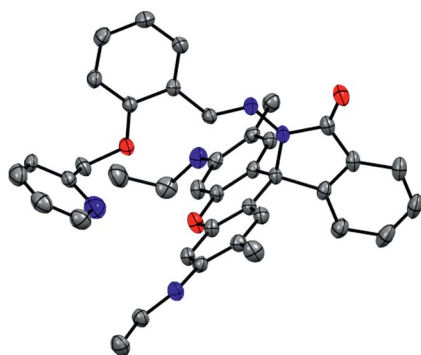


Figure 1. ORTEP view of ligand L<sup>3</sup> with ellipsoids drawn at the 30% probability level. Symmetry code: a = x, y, z; b = -x, 1/2 + y, 1/2 - z; c = -x, -y, -z; d = x, 1/2 - y, 1/2 + z.

The emission spectra of L<sup>3</sup> and its fluorescence titration with Hg<sup>2+</sup> were also performed in MeCN/water solution (6:4, v/v, HEPES buffer, pH 7.1; Figure 3A). On gradual addition of Hg<sup>2+</sup> (0–35 μM) to the non-fluorescent solution of L<sup>3</sup> (7 μM), a 252-fold enhancement in fluorescence intensity at 553 nm was observed following excitation at 508 nm, which also suggests the opening of the spiro-lactam ring in L<sup>3</sup> on coordination to the Hg<sup>2+</sup> ion.<sup>[19]</sup> The non-linear least-squares fit of the fluorescence titration data of L<sup>3</sup> (7.0 μM) with Hg<sup>2+</sup> (0–35 μM) gives an association constant *K* of (6.48 ± 1.84) × 10<sup>5</sup> M<sup>-1</sup> (see Figure S2 in the Supporting Information).

The detection of Hg<sup>2+</sup> was not perturbed by the presence of biologically abundant Na<sup>+</sup>, K<sup>+</sup>, Ca<sup>2+</sup> and Mg<sup>2+</sup> ions. Similarly, several transition-metal ions, namely Cr<sup>3+</sup>, Mn<sup>2+</sup>, Fe<sup>2+</sup>, Fe<sup>3+</sup>, Co<sup>2+</sup>, Cu<sup>2+</sup>, Ni<sup>2+</sup> and Zn<sup>2+</sup>, and heavy-metal ions, like Cd<sup>2+</sup>, Pb<sup>2+</sup> and Ag<sup>+</sup>, did not show any significant

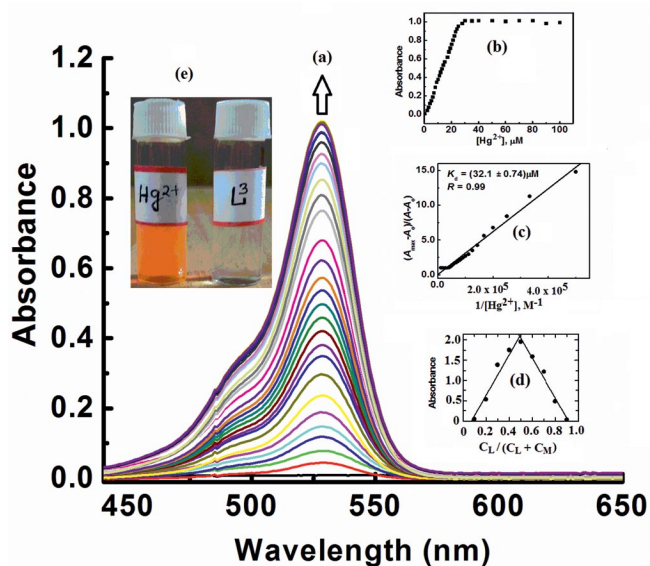


Figure 2. (A) Change in the absorption spectra of L<sup>3</sup> (20 μM) upon addition of Hg<sup>2+</sup> in HEPES buffer at pH 7.1 in H<sub>2</sub>O/MeCN (4:6, v/v) at 25 °C with [Hg<sup>2+</sup>] = 0–100 μM. (B) Plot of the absorbance at 529 nm vs. [Hg<sup>2+</sup>]. (C) Benesi–Hilderband plot of (A<sub>max</sub> - A<sub>0</sub>)/(A - A<sub>0</sub>) vs. 1/[Hg<sup>2+</sup>]. (D) Job's plot. (E) Photographs of solutions of L<sup>3</sup> and the L<sup>3</sup>-Hg<sup>2+</sup> complex in MeCN/water.

colour or spectral change under identical conditions (Figure 4, A,B). For practical applications, the appropriate pH conditions for successful operation of the sensor were evaluated. No obvious fluorescence emission of L<sup>3</sup> was observed between pH 5 and 12, which suggests that the spiro-lactam form of L<sup>3</sup> is stable over this wide range of pH and can work well under physiological pH conditions (Figure 3, B).

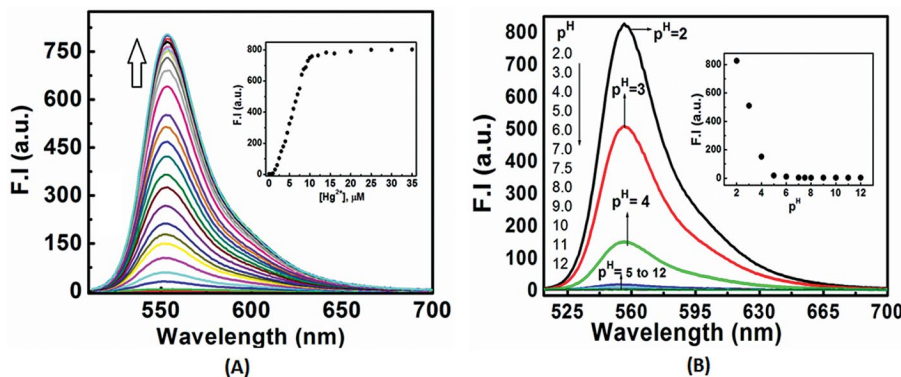


Figure 3. (A) Change in the fluorescence intensity of  $L^3$  ( $7 \mu\text{M}$ ) upon addition of  $\text{Hg}^{2+}$  in HEPES buffer at pH 7.1 in  $\text{H}_2\text{O}/\text{MeCN}$  (4:6, v/v) at  $25^\circ\text{C}$  with  $[\text{Hg}^{2+}] = 0\text{--}35 \mu\text{M}$  ( $\lambda_{\text{ex}} = 508 \text{ nm}$ ); inset: plot of fluorescence intensity (at  $553 \text{ nm}$ ) vs.  $[\text{Hg}^{2+}]$ . (B) pH–stability study of the sensor  $L^3$  ( $6 \mu\text{M}$ ); inset: fluorescence intensity vs. pH plot at  $556 \text{ nm}$ .

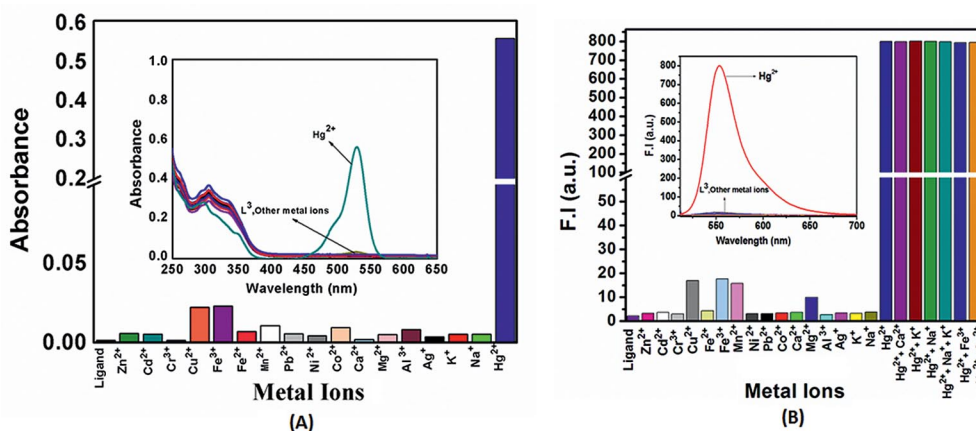


Figure 4. (A) UV/Vis spectral study of the selective binding of  $L^3$  ( $10 \mu\text{M}$ ) towards  $\text{Hg}^{2+}$  over other metal ions (5 equiv.). (B) Fluorescence study of the selective binding of  $L^3$  ( $7 \mu\text{M}$ ) towards  $\text{Hg}^{2+}$  over other metal ions (5 equiv.).

A short response time and reversible response are also necessary for a fluorescent sensor to monitor  $\text{Hg}^{2+}$  ions in practical applications. The time dependence of the response of  $L^3$  to the  $\text{Hg}^{2+}$  ion was investigated and the results reveal that the recognition event could occur almost immediately upon mixing ( $\leq 1 \text{ min}$ ; see Figure S3 in the Supporting Information). The reversible binding of  $L^3$  to  $\text{Hg}^{2+}$  was investigated in the same solvent system as used in the absorption and fluorescence titrations (see Figure S4 in the Supporting Information). Various anions, for example,  $\text{SO}_4^{2-}$ ,  $\text{SO}_3^{2-}$ ,  $\text{NO}_3^-$ ,  $\text{PO}_4^{3-}$ ,  $\text{CO}_3^{2-}$ ,  $\text{S}^{2-}$ ,  $\text{Cl}^-$ ,  $\text{F}^-$ ,  $\text{Br}^-$ ,  $\text{I}^-$ ,  $\text{OAc}^-$  and  $\text{N}_3^-$ , were introduced into the solution containing  $L^3$  and  $\text{Hg}^{2+}$  and the changes in their absorption and fluorescence intensities were monitored after 3 min. The results show that anions like  $\text{I}^-$  and  $\text{S}^{2-}$  have a strong affinity towards  $\text{Hg}^{2+}$  and their binding constants may be much higher than that of  $L^3$ . This causes demetallation of  $\text{Hg}^{2+}$  from the complex and regeneration of the spiro-lactam ring with bleaching of the absorption band at  $529 \text{ nm}$  and the emission band at around  $553 \text{ nm}$ . The quantum yield of the  $L^3\text{--Hg}^{2+}$  complex was determined to be  $\Phi = 0.783$  (with rhodamine 6G used as a standard), whereas the free ligand is non- or very weakly fluorescent with a very negligible absorption band at  $529 \text{ nm}$ . The limit of detection (LOD) of  $\text{Hg}^{2+}$  was deter-

mined by the  $3\sigma$  method<sup>[20]</sup> and found to be as low as  $9.28 \text{ ng L}^{-1}$ . All these findings indicate that  $L^3$  behaves as a good example of an ideal chemosensor for  $\text{Hg}^{2+}$  recognition.

The mechanistic pathway proposed for the formation of the  $L^3\text{--Hg}^{2+}$  complex by opening of the spiro-lactam ring was established through IR and  $^1\text{H}$  and  $^{13}\text{C}$  NMR studies. The IR study revealed that the characteristic stretching frequency of the amidic “ $\text{C}=\text{O}$ ” of the rhodamine moiety at  $1710 \text{ cm}^{-1}$  is shifted to a lower wavenumber ( $1649 \text{ cm}^{-1}$ ) in the presence of 1.2 equiv. of  $\text{Hg}^{2+}$  (Figure 5). This large shift signifies a strong polarization of the  $\text{C}=\text{O}$  bond upon efficient binding to the  $\text{Hg}^{2+}$  ion and in fact indicates cleavage of this bond. Also, the  $^1\text{H}$  NMR spectra show the ring protons (f and g; see the labelling in Figure S5 in the Supporting Information) of the rhodamine moiety are shifted downfield in the presence of 1.2 equiv. of  $\text{Hg}^{2+}$  ions. The “p” proton shows an upfield shift mainly due to an increase in electron density arising from the opening of the spiro-lactam ring. The complex signal pattern of the other aromatic protons also indicates the involvement of the pyridine moiety of the receptor unit of  $L^3$  in the binding of  $\text{Hg}^{2+}$ . Also, the disappearance from the  $^{13}\text{C}$  NMR spectrum of the signal at  $\delta = 64.79 \text{ ppm}$  for the tertiary carbon ( $\text{sp}^3$ -

hybridized) of the spiro-lactam ring of  $L^3$  (labelled as C4, see Figure 6) upon addition of 1.2 equiv. of  $Hg^{2+}$  convincingly supports the opening of the spiro-lactam ring and coordination through the O atom of the -CONH group of the rhodamine moiety to the  $Hg^{2+}$  ion.<sup>[21]</sup>

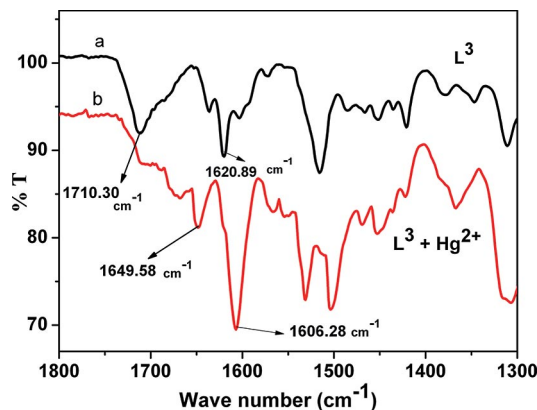


Figure 5. IR spectra of  $L^3$  and  $L^3$ - $Hg^{2+}$  in  $CH_3CN$ .

The INHIBIT logic gate involves a particular combination of the LOGIC functions AND and NOT. For our system we can make a correlation by taking two input signals, namely input 1 ( $Hg^{2+}$ ) and input 2 ( $I^-$ ), along with fluorescence signal of the probe  $L^3$  ( $5 \mu M$ ) at 553 nm as the output.

For the input, the presence and absence of  $Hg^{2+}$  and  $I^-$  are assigned as 1 (ON state) and 0 (OFF state), respectively. For output, we assign the enhanced fluorescence of  $L^3$  as 1 (ON state) and the quenched fluorescence as 0 (OFF state; see the Truth Table in Figure 7, B). In the absence of both inputs ( $Hg^{2+}$  or  $I^-$ ),  $L^3$  remains in the OFF-state form. Input 1 leads to significant fluorescence enhancement through its interaction with the free receptor in its occupied state leading to the ON-state form, but the interaction of input 2 with its corresponding receptor leads to the OFF-state form, thereby implementing the necessary NOT gate. The

probe acts in parallel with the fluorescence output signals, which implements the required AND function. The combination of both inputs leads to fluorescence quenching as output 0, in accordance with the Truth Table in Figure 7 (B). Therefore monitoring the fluorescence at 553 nm upon addition of  $Hg^{2+}$ ,  $I^-$  and a mixture of the two satisfies an INHIBIT logic gate function (Figure 7).

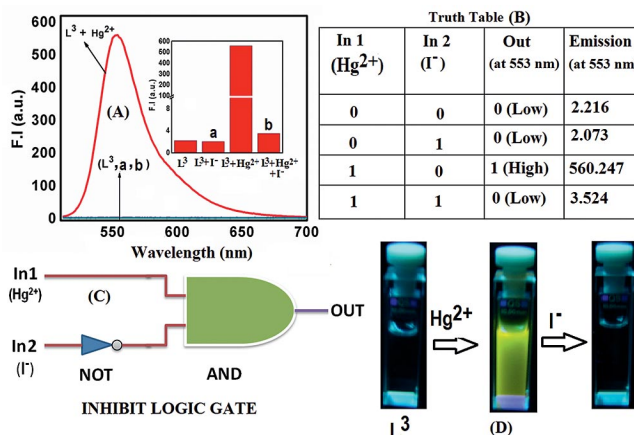


Figure 7. (A) Output signals (at 553 nm) of the logic gate in the presence of different inputs. (B) Corresponding Truth Table of the logic gate. (C) General representation of an INHIBIT gate. (D) UV-exposed photographs of  $L^3$ ,  $L^3$ - $Hg^{2+}$  and a mixture of  $L^3$ - $Hg^{2+}$  +  $I^-$  in  $MeCN/H_2O$  (6:4, v/v, pH 7.1, HEPES buffer) solvent.

The intracellular  $Hg^{2+}$  imaging behaviour of  $L^3$  was studied by using HeLa cells in conjunction with fluorescence microscopy. After incubation with  $L^3$ , the cells displayed no intracellular fluorescence (Figure 8, B). However, the cells exhibited intense fluorescence when a solution of  $Hg(ClO_4)_2$  (10–50  $\mu M$ ) was added to the  $L^3$  pre-incubated cells (Figure 8, C–E). However, the intense fluorescence was strongly suppressed when KI (100  $\mu M$ ) was also added to this medium. Because KI shows a strong scavenging action

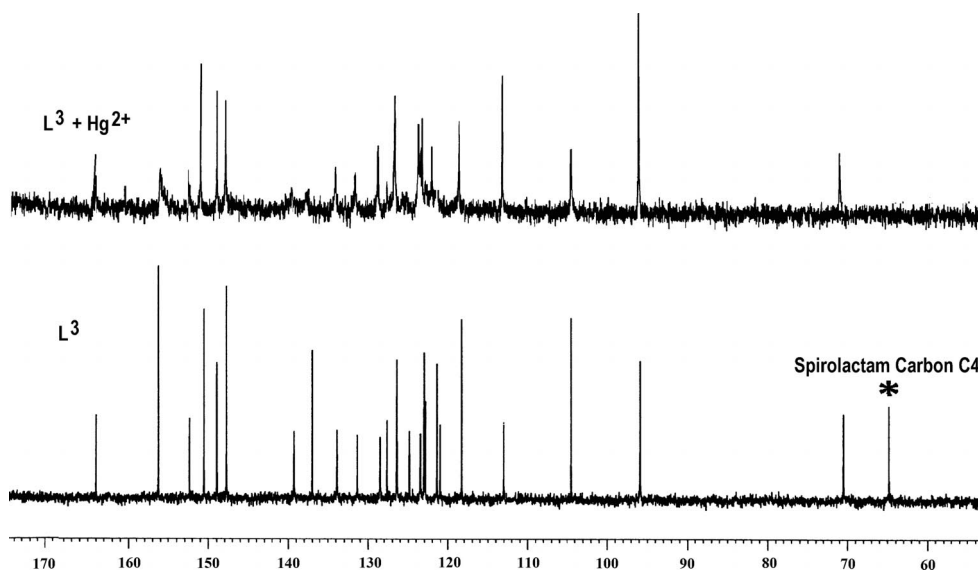


Figure 6.  $^{13}C$  NMR spectra of  $L^3$  and  $L^3$ - $Hg^{2+}$  in  $[D_6]dmsO$ .

on  $\text{Hg}^{2+}$ , the sensor was competitively inhibited from binding to  $\text{Hg}^{2+}$ , and so the fluorescence almost disappeared (Figure 8, F). This confirms the ability of the  $\text{L}^3$  to sense  $\text{Hg}^{2+}$  ions in biological systems under physiological conditions. Also,  $\text{L}^3$  can effectively be used to monitor changes in the intracellular concentration of  $\text{Hg}^{2+}$  ions under different biological conditions, particularly because of its relatively low cytotoxicity up to 8 h (Figure 9).

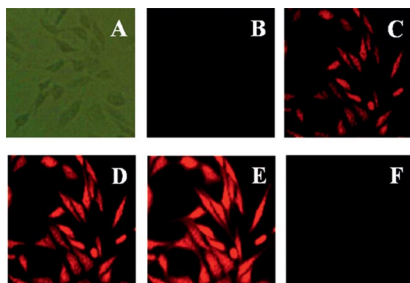


Figure 8. (A) Phase contrast. (B) Fluorescence image of HeLa cells in the absence of chemosensor  $\text{L}^3$ . Chemosensor  $\text{L}^3$  ( $10 \mu\text{M}$ )-incubated cells washed with PBS (pH 7.2) and exposed to increasing concentrations of extracellular  $\text{Hg}^{2+}$  ions: (C) 10, (D) 20 and (E)  $50 \mu\text{M}$ . (F) Image E + KI ( $100 \mu\text{M}$ ). For all imaging, the samples were excited at 508 nm.

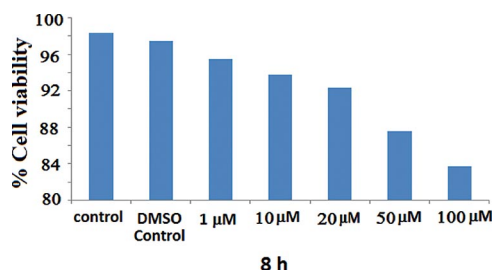


Figure 9. Cell viability (determined by the MTT assay) of HeLa cells treated with different concentrations of chemosensor  $\text{L}^3$  for 8 h.

## Conclusions

We have designed and synthesized a new rhodamine-based chromo-/fluorogenic dual signalling probe for selective recognition of  $\text{Hg}^{2+}$ , which has been characterized by  $^1\text{H}$  and  $^{13}\text{C}$  NMR, IR, ESI-MS and single-crystal X-ray diffraction. The rhodamine-based ligand  $\text{L}^3$  displays visible colorimetric as well as fluorogenic properties on selective binding to  $\text{Hg}^{2+}$  with a 252-fold enhancement of the fluorescence. Benesi–Hilderband analysis of the absorption titration data gives  $K_d = (32.01 \pm 0.74) \mu\text{M}$  with 1:1 complexation. Owing to its solubility in  $\text{MeCN}/\text{H}_2\text{O}$  and cell permeability it could be used for in vitro/in vivo cell-imaging of  $\text{Hg}^{2+}$  with no or negligible cytotoxicity. The detection limit of  $\text{Hg}^{2+}$  was calculated by the  $3\sigma$  method to be  $9.28 \text{ ng L}^{-1}$ . Moreover, reversible binding of  $\text{L}^3$  to  $\text{Hg}^{2+}$  may be useful in real-time applications, which is superior to irreversible binding of a probe towards a metal ion. Thus, the “OFF–ON–OFF” fluorescence sensing behaviour observed in the presence of  $\text{Hg}^{2+}$  and  $\text{I}^-$  strengthens the poten-

tial applications of the  $\text{L}^3$ – $\text{Hg}^{2+}$  system as a device with logic gate functions and therefore shows advantages for the development of new-generation digital devices.

## Experimental Section

**Materials and Instruments:** Steady-state fluorescence studies were carried out with a Shimadzu (Model RF-5301PC) and Horiba–Jobin–Yvon Fluoromax-3 spectrofluorimeters. UV/Vis absorption spectra were recorded with an Agilent 8453 diode array spectrophotometer. NMR spectra were recorded with a Bruker spectrometer at 300 MHz. The ESI-MS<sup>+</sup> spectra were recorded with a Qtof Micro YA263 mass spectrometer.

All solvents used for synthesis were of reagent-grade (Merck) unless otherwise mentioned. For spectroscopic (UV/Vis and fluorescence) studies HPLC-grade  $\text{MeCN}$  and double-distilled water were used. Rhodamine 6G hydrochloride, 2-chloromethylpyridine and metal salts such as the perchlorates of  $\text{Na}^+$ ,  $\text{K}^+$ ,  $\text{Ca}^{2+}$ ,  $\text{Fe}^{2+}$ ,  $\text{Co}^{2+}$ ,  $\text{Ni}^{2+}$ ,  $\text{Zn}^{2+}$ ,  $\text{Pb}^{2+}$ ,  $\text{Cd}^{2+}$ ,  $\text{Hg}^{2+}$  and  $\text{Cu}(\text{NO}_3)_2 \cdot 2\text{H}_2\text{O}$  were purchased from Sigma–Aldrich and used as received. All other compounds were purchased from commercial sources and used as received.

**Preparation of Rhodamine 6G Hydrazide ( $\text{L}^1$ ):** Rhodamine 6G hydrazide was prepared according to a literature method.<sup>[22]</sup>

**Preparation 2-(Pyridin-2-ylmethoxy)benzaldehyde ( $\text{L}^2$ ):**  $\text{L}^2$  was prepared by a modification of a literature procedure.<sup>[23]</sup> Salicylaldehyde (10 mmol, 1.23 g) and  $\text{K}_2\text{CO}_3$  (18 mmol, 2.52 g) were added to dry  $\text{MeCN}$  (60 mL), and the mixture was heated at reflux for 40 min. 2-Picolyl chloride (11.5 mmol, 1.89 g) and a catalytic amount of KI (0.15 g) was then added to the above reaction mixture, which was heated at reflux for a further 12 h. Then the mixture was cooled and filtered. The filtrate was evaporated to one third of its initial volume and diluted with water (40 mL). Then the pH of the solution was adjusted to 4 by the addition of 1 M HCl and extracted with dichloromethane (dcm;  $2 \times 40 \text{ mL}$ ). The pH of the aqueous solution was then adjusted to 8 by the addition of 4.0 M  $\text{Na}_2\text{CO}_3$  solution and extracted with dcm ( $3 \times 40 \text{ mL}$ ). Then the combined organic phase after drying with anhydrous  $\text{Na}_2\text{SO}_4$  was evaporated to dryness under reduced pressure to give a pale-yellow solid residue. The crude solid product was recrystallized in  $\text{MeOH}/\text{dcm}$  (8:2, v/v) to give the desired NMR-pure product as an off-white crystalline solid (66% yield), m.p.  $69.4 \text{ }^\circ\text{C}$ .  $^1\text{H}$  NMR ( $\text{CDCl}_3$ ):  $\delta = 10.62$  (s, 1 H), 8.62 (dd, 1 H), 7.76 (td, 1 H), 7.54 (m, 2-H), 7.29 (ddd, 1 H), 7.07 (m, 2 H), 5.33 (s, 2 H) ppm.  $^{13}\text{C}$  NMR ( $\text{CDCl}_3$ ):  $\delta = 189.53, 160.59, 156.32, 149.35, 137.04, 135.98, 128.85, 125.16, 123.01, 121.26, 121.21, 113.04, 71.10$  ppm. IR:  $\tilde{\nu} = 1690$  (CHO), 1253 (aliphatic C–O)  $\text{cm}^{-1}$ . MS (ES<sup>+</sup>):  $m/z = 214.07$  [ $\text{L} + \text{H}$ ]<sup>+</sup>.  $\text{C}_{13}\text{H}_{11}\text{NO}_2$  (213.24): calcd. C 73.19, H 5.21, N 6.62; found C 73.37, H 5.09, N 6.58.

**Preparation of Probe  $\text{L}^3$ :**  $\text{L}^2$  (1.1 mmol, 0.234 g) in  $\text{MeOH}$  (10 mL) was added dropwise over 30 min to a methanolic solution (30 mL) of  $\text{L}^1$  (1 mmol, 0.428 g) containing 1 drop of acetic acid under hot (ca.  $50$ – $60 \text{ }^\circ\text{C}$ ) conditions. Then the reaction mixture was stirred for around 6 h at room temperature. An off-white precipitate was formed, which was collected by filtration. The residue was washed thoroughly with cold methanol to isolate  $\text{L}^3$  in pure form in 84% yield. Single crystals of  $\text{L}^3$  were obtained by recrystallization in  $\text{dcm}/\text{MeCN}$  (1:1, v/v), m.p.  $222.2 \text{ }^\circ\text{C}$ .  $^1\text{H}$  NMR ( $\text{CDCl}_3$ ):  $\delta = 8.76$  (s, 1 H), 8.57 (s, 1 H), 7.99–8.05 (m, 2 H), 7.80 (t, 1 H), 7.46 (t, 2-H), 7.22–7.26 (s, 2-H), 7.16 (t, 1-H), 7.06 (t, 1 H), 6.90 (t, 1 H), 6.74 (d, 1 H), 6.39 (s, 2 H), 6.30 (s, 2 H), 5.11 (s, 1 H), 3.43 (br., 2 H), 3.11 (q, 4 H), 1.87 (s, 6 H), 1.25 (t, 6 H) ppm.  $^{13}\text{C}$ NMR ( $[\text{D}_6]$ -

dmsO):  $\delta$  = 163.99, 156.3, 152.32, 150.5, 148.94, 147.7, 139.3, 137.0, 134.0, 127.7, 126.5, 124.9, 123.0, 122.9, 121.5, 121.04, 118.3, 113.44, 104.44, 95.88, 70.47, 64.79, 37.5, 16.94, 14.06 ppm. MS (ES<sup>+</sup>):  $m/z$  = 624.22 [L + H]<sup>+</sup>. IR:  $\tilde{\nu}$  = 1710 (spiro-lactam amide keto), 1621 (C=N), 1261 (aliphatic C–O) cm<sup>-1</sup>. C<sub>39</sub>H<sub>37</sub>N<sub>5</sub>O<sub>3</sub> (623.75): calcd. C 75.11, H 5.99, N 11.23; found C 74.98, H 5.85, N 11.76.

### Cell Imaging Experiment and Cytotoxicity Studies

**Cell Culture:** The HeLa cell line of human cervical cancer origin was obtained from the National Center for Cell Science, Pune, India, and used throughout the study. The cells were cultured in Dulbecco's modified eagle medium (DMEM; Gibco BRL) supplemented with 10% fetal bovine serum (FBS; Gibco BRL) and a 1% antibiotic mixture containing penicillin, streptomycin and neomycin (PSN; Gibco BRL) at 37 °C in a humidified incubator with 5% CO<sub>2</sub>. The cells were grown to 80–90% confluence, harvested with 0.025% trypsin (Gibco BRL) and 0.52 mM edta (Gibco BRL) in phosphate-buffered saline (PBS), plated at the desired cell concentration and allowed to re-equilibrate for 24 h before any treatment.

**Cell-Imaging Study:** Cells were rinsed with PBS and incubated with DMEM containing L<sup>3</sup> making the final concentration up to 10  $\mu$ M in DMEM; the stock solution (1 mM) was prepared by dissolving L<sup>3</sup> in the mixed solvent (dmsO/water = 1:9, v/v) for 30 min at 37 °C. After incubation, bright field and fluorescence images of the HeLa cells were taken with a Leica DMLS fluorescence microscope with an objective lens of 20 $\times$  magnification. Fluorescence images were taken of the HeLa cells incubated with 10  $\mu$ M L<sup>3</sup> for 30 min and after the addition of different concentrations (10–50  $\mu$ M) of Hg<sup>2+</sup> ions and KI (100  $\mu$ M).

**Cell Cytotoxicity Assay:** To test the cytotoxicity of L<sup>3</sup>, the 3-(4,5-dimethylthiazol-2-yl)-2,5-diphenyltetrazolium bromide (MTT) assay was performed following the procedure described previously.<sup>[24]</sup> After treatment with 1, 10, 20, 50 and 100  $\mu$ M L<sup>3</sup> for 8 h, 10  $\mu$ L of MTT solution (10 mg/mL PBS) was added to each well of a 96-well culture plate and again incubated at 37 °C for a period of 3 h. All media were removed from the wells and acidic isopropyl alcohol (100  $\mu$ L) was added to each well. The intracellular formazan crystals (blue-violet) formed were solubilized with 0.04 N acidic isopropyl alcohol and the absorbance of the solution was measured at 595 nm with a Thermo Multi Scan EX microplate reader. The cell viability was expressed as the optical density ratio of the treated sample and control. Values are expressed as the mean of three independent experiments. The cell cytotoxicity was calculated as the % cell cytotoxicity = 100% – % cell viability.

CCDC-926524 contains the supplementary crystallographic data for this paper. These data can be obtained free of charge from The Cambridge Crystallographic Data Centre via [www.ccdc.cam.ac.uk/data\\_request/cif](http://www.ccdc.cam.ac.uk/data_request/cif).

**Supporting Information** (see footnote on the first page of this article): IR, NMR, MS, UV/Vis spectra, fluorescence titration data, X-ray crystal data, photographs of solutions of L<sup>3</sup> with different metal ions.

### Acknowledgments

Financial support from the Department of Science and Technology (DST), Government of India, New Delhi (ref. number SR/S1/IC-20/2012) and the Council of Scientific and Industrial Research (CSIR), New Delhi [ref. number 01(2490)/11/EMR-II] is gratefully acknowledged. T. M. and M. D. acknowledge fellowships from the

University Grants Commission (UGC), New Delhi (UGC-NET). S. K. M. is grateful to the DST for partial financial support through the PURSE Program.

- [1] a) X. Chen, X. Tian, I. Shin, J. Yoon, *Chem. Soc. Rev.* **2011**, *40*, 4783–4804; b) A. W. Czarnik, *Fluorescent Chemosensors for Ion and Molecule Recognition*, American Chemical Society, Washington, DC, **1993**; c) B. Valeur, I. Leray, *Coord. Chem. Rev.* **2000**, *205*, 3–40; d) R. Martínez-Máñez, F. Sancenón, *Chem. Rev.* **2003**, *103*, 4419–4476; e) L. Basabe-Desmonts, D. N. Reinhoudt, M. Crego-Calama, *Chem. Soc. Rev.* **2007**, *36*, 993–1017.
- [2] H. N. Kim, W. X. Ren, J. S. Kim, J. Yoon, *Chem. Soc. Rev.* **2012**, *4*, 3210–3244.
- [3] a) F. Di Natale, A. Lancia, A. Molino, M. Di Natale, D. Karatza, D. Musmarra, *J. Hazard. Mater.* **2006**, *132*, 220; b) T. Takeuchi, N. Morikawa, H. Matsumoto, Y. Shiraishi, *Acta Neuropathol.* **1962**, *2*, 40–57; c) M. Harada, *Crit. Rev. Toxicol.* **1995**, *25*, 1–24; d) C. T. Walsh, M. D. Distefano, M. J. Moore, L. M. Shewchuk, G. L. Verdine, *FASEB J.* **1988**, *2*, 124–130.
- [4] a) E. M. Nolan, S. J. Lippard, *Chem. Rev.* **2008**, *108*, 3443–3480; b) N. E. Molan, S. J. Lippard, *J. Am. Chem. Soc.* **2003**, *125*, 14270–14271; c) E. M. Nolan, M. E. Racine, S. J. Lippard, *Inorg. Chem.* **2006**, *45*, 2742–2749; d) J. V. Ros-lis, M. D. Marcos, R. Martinez-Manez, K. Rurack, J. Soto, *Angew. Chem.* **2005**, *117*, 4479; *Angew. Chem. Int. Ed.* **2005**, *44*, 4405–4407; e) A. Caballero, R. Martinez, V. Lloveras, I. Ratera, J. Vidal-Gancedo, K. Wurst, A. Tarraga, P. Molina, J. Veciana, *J. Am. Chem. Soc.* **2005**, *127*, 15666–15667; f) X. Guo, X. Qian, L. Jia, *J. Am. Chem. Soc.* **2004**, *126*, 2272–2273; g) M. J. Vello, N. S. Finney, *J. Am. Chem. Soc.* **2005**, *127*, 10124–10125; h) A. Coskun, E. U. Akkaya, *J. Am. Chem. Soc.* **2006**, *128*, 14474–14475; i) S. Yoon, E. W. Miller, Q. He, P. H. Do, C. J. Chang, *Angew. Chem.* **2007**, *119*, 6778; *Angew. Chem. Int. Ed.* **2007**, *46*, 6658–6661; j) A. B. Descalzo, R. Martinez-Manez, R. Radeglia, K. Rurack, J. Soto, *J. Am. Chem. Soc.* **2003**, *125*, 3418–3419; k) M. Suresh, A. Shrivastav, S. Mishra, E. Suresh, A. Das, *Org. Lett.* **2008**, *10*, 3010–3016; l) M. Suresh, A. Ghosh, A. Das, *Chem. Commun.* **2008**, 3906–3908.
- [5] a) Y. Gao, S. De Galan, A. De Brauwere, W. Baeyens, M. Leermakers, *Talanta* **2010**, *82*, 1919–1923; b) M. J. da Silva, A. P. S. Paim, M. F. Pimentel, M. L. Cervera, M. de la Guardia, *Anal. Chim. Acta* **2010**, *667*, 43–48.
- [6] a) F. Moreno, T. Garcia-Barrera, J. L. Gomez-Ariza, *Analyst* **2010**, *135*, 2700–2705; b) M. V. B. Krishna, K. Chandrasekaran, D. Karunasagar, *Talanta* **2010**, *81*, 462–472; c) W. R. L. Cairns, M. Ranaldo, R. Hennebelle, C. Turetta, G. Capodaglio, C. F. Ferrari, A. Dommergue, P. Cescon, C. Barbante, *Anal. Chim. Acta* **2008**, *622*, 62–69.
- [7] X. Chai, X. Chang, Z. Hu, Q. He, Z. Tu, Z. Li, *Talanta* **2010**, *82*, 1791–1796.
- [8] a) X. Fu, X. Chen, Z. Guo, C. Xie, L. Kong, J. Liu, X. Huang, *Anal. Chim. Acta* **2011**, *685*, 21–28; b) F. Wang, X. Wei, C. Wang, S. Zhang, B. Ye, *Talanta* **2010**, *80*, 1198–1204.
- [9] a) X. Guo, X. Qian, L. Jia, *J. Am. Chem. Soc.* **2004**, *126*, 2272–2273; b) J. Wang, X. Qian, *Chem. Commun.* **2006**, 109–111; c) M. Yuan, Y. Li, J. Li, C. Li, X. Liu, J. Lv, J. Xu, H. Liu, S. Wang, D. Zhu, *Org. Lett.* **2007**, *9*, 2313–2316; d) A. Coskun, M. D. Yilmaz, E. U. Akkaya, *Org. Lett.* **2007**, *9*, 607–609; e) M. H. Lee, S. W. Lee, S. H. Kim, C. Kang, J. S. Kim, *Org. Lett.* **2009**, *11*, 2101–2104; f) J. Fan, K. Guo, X. Peng, J. Du, J. Wang, S. Sun, H. Li, *Sens. Actuators B* **2009**, *142*, 191–196; g) V. Bhalla, R. Tejpal, M. J. Kumar, A. Sethi, *Inorg. Chem.* **2009**, *48*, 11677–11684; h) K. G. Vaswani, M. D. Keranen, *Inorg. Chem.* **2009**, *48*, 5797–5800; i) N. Wanichacheva, M. Siriprumpoonthum, A. Kamkaew, K. Grudpan, *Tetrahedron Lett.* **2009**, *50*, 1783–1786; j) J. Du, J. Fan, X. Peng, P. Sun, J. Wang, H. Li, S. Sun, *Org. Lett.* **2010**, *12*, 476–479; k) W. Shi, S. Sun, X. Li, H. Ma, *Inorg. Chem.* **2010**, *49*, 1206–1210; l) S. Atilgan, T. Ozdemir, E. U. Akkaya, *Org. Lett.* **2010**, *12*, 4792–4795; m)

- O. A. Bozdemir, R. Guliyev, O. Buyukcakir, S. Selcuk, S. Kolemen, G. Gulseren, T. Nalbantoglu, H. Boyaci, E. U. Akkaya, *J. Am. Chem. Soc.* **2010**, *132*, 8029–8036.
- [10] a) M. Yuan, Y. Li, J. Li, C. Li, X. Liu, J. Lv, J. Xu, H. Liu, S. Wang, D. Zhu, *Org. Lett.* **2007**, *9*, 2313–2316; b) M. Zhu, M. Yuan, X. Liu, J. Xu, J. Lv, C. Huang, H. Liu, Y. Li, S. Wang, D. Zhu, *Org. Lett.* **2004**, *6*, 1489–1492; c) H.-K. Chen, C.-Y. Lu, H.-J. Cheng, S.-J. Chen, C.-H. Hu, A.-T. Wu, *Carbohydr. Res.* **2010**, *345*, 2557–2561; d) J. Hu, M. Zhang, B. L. Yu, Y. Ju, *Bioorg. Med. Chem. Lett.* **2010**, *20*, 4342–4345; e) A. Thakur, S. Sardar, S. Ghosh, *Inorg. Chem.* **2011**, *50*, 7066–7073; f) B. Nisar Ahamed, I. Ravikumar, P. Ghosh, *New J. Chem.* **2009**, *33*, 1825–1828; g) J. S. Kim, S. Y. Lee, J. Yoon, J. Vicens, *Chem. Commun.* **2009**, 4791–4802; h) S.-M. Cheung, W.-H. Chan, *Tetrahedron* **2006**, *62*, 8379–8383; i) E. M. Nolan, S. J. Lippard, *Chem. Rev.* **2008**, *108*, 3443–3480; j) H. N. Kim, M. H. Lee, H. J. Kim, J. S. Kim, J. Yoon, *Chem. Soc. Rev.* **2008**, *37*, 1465–1472; k) J. Wang, X. Qian, J. Cui, *J. Org. Chem.* **2006**, *71*, 4308–4311; l) A. Coskun, M. D. Yilmaz, E. U. Akkaya, *Org. Lett.* **2007**, *9*, 607–609; m) A. Cabellero, A. Espinosa, A. Tarraga, P. Molina, *J. Org. Chem.* **2008**, *73*, 5489–5497; n) J. Wang, B. Liu, *Chem. Commun.* **2008**, 4759–4761; o) Y. Zhao, B. Zheng, J. Du, D. Xiao, L. Yang, *Talanta* **2011**, *85*, 2194–2201; p) J. F. Zhang, J. S. Kim, *Anal. Sci.* **2009**, *25*, 1271–1281; q) M. Suresh, A. Ghosh, A. Das, *Chem. Commun.* **2008**, 3906–3908; r) L. Jiang, L. Wang, B. Zhang, G. Yin, R.-Y. Wang, *Eur. J. Inorg. Chem.* **2010**, 4438–4443.
- [11] a) D. S. McClure, *J. Chem. Phys.* **1952**, *20*, 682–686; b) J. F. Zhang, J. S. Kim, *Anal. Sci.* **2009**, *25*, 1271–1281; c) J. Yoon, N. E. Ohler, D. H. Vance, W. D. Aumiller, A. W. Czarnik, *Tetrahedron Lett.* **1997**, *38*, 3845–3848.
- [12] a) H. M. Kim, B. R. Cho, *Acc. Chem. Res.* **2009**, *42*, 863–872; b) S.-K. Ko, Y.-K. Yang, J. Tae, I. Shin, *J. Am. Chem. Soc.* **2006**, *128*, 14150–14155; c) H. Yang, Z. Zhou, K. Huang, M. Yu, F. Li, T. Yi, C. Huang, *Org. Lett.* **2007**, *9*, 4729–4732.
- [13] a) J. R. Lakowicz, *Principles of Fluorescence Spectroscopy*, 3rd ed., Springer, New York, **2006**, p. 67–69; b) G. Grynkiewicz, M. Poenie, R. Y. J. Tsien, *Biol. Chem.* **1985**, *260*, 3440–3450; c) A. Minta, R. Y. J. Tsien, *Biol. Chem.* **1989**, *264*, 19449–19457; d) E. Kimura, T. Koike, *Chem. Soc. Rev.* **1998**, *27*, 179–184; e) Y. K. Yang, K.-J. Yook, J. Tae, *J. Am. Chem. Soc.* **2005**, *127*, 16760–16761.
- [14] R. P. Haugland, *The Handbook: A Guide to Fluorescent Probes and Labeling Technologies*, 10th ed., Invitrogen Corp., Carlsbad, CA, **2005**.
- [15] a) V. Balzani, A. Credi, F. M. Raymo, J. F. Stoddart, *Angew. Chem.* **2000**, *112*, 3484–3530; b) J. Andrasson, U. Pischel, *Chem. Soc. Rev.* **2010**, *39*, 174–188; c) K. Szacilowski, *Chem. Rev.* **2008**, *108*, 3481–3548; d) D. Margulies, G. Melman, A. Shanzer, *J. Am. Chem. Soc.* **2006**, *128*, 4865–4871.
- [16] a) A. P. de Silva, H. Q. N. Gunaratne, C. P. McCoy, *Nature* **1993**, *364*, 42–44; b) M. N. Stojanovic, T. E. Mitchell, D. Stefanovic, *J. Am. Chem. Soc.* **2002**, *124*, 3555–3561; c) X. Guo, D. Zhang, T. Wang, D. Zhu, *Chem. Commun.* **2003**, 914–915; d) X. F. Guo, D. Q. Zhang, G. X. Zhang, D. B. Zhu, *J. Phys. Chem. B* **2004**, *108*, 11942–11945; e) D. H. Qu, F. Y. Ji, Q. C. Wang, H. Tian, *Adv. Mater.* **2006**, *18*, 2035–2038; f) A. P. de Silva, N. D. McCenaghan, *Chem. Eur. J.* **2004**, *10*, 574–586; g) D. Zhang, J. Su, X. Ma, H. Tian, *Tetrahedron* **2008**, *64*, 8515–8521; h) S. H. Lee, J. Y. Kim, S. K. Kim, J. H. Lee, J. S. Kim, *Tetrahedron* **2004**, *60*, 5171–5176; i) M. Kumar, R. Kumar, V. Bhalla, *Tetrahedron Lett.* **2010**, *51*, 5559–5562; j) M. Kumar, R. Kumar, V. Bhalla, *Chem. Commun.* **2009**, 7384–7386; k) M. Kumar, A. Dhir, V. Bhalla, *Org. Lett.* **2009**, *11*, 2567–2570; l) X. Meng, W. Zhu, Q. Zhang, Y. Feng, W. Tan, H. Tian, *J. Phys. Chem. B* **2008**, *112*, 15636–15645; m) L. Fabbrizzi, M. Licchelli, P. Pallavicini, *Acc. Chem. Res.* **1999**, *32*, 846–853; n) Z. Dong, X. Tian, Y. Chen, J. Hou, J. Ma, *RSC Adv.* **2013**, *3*, 2227–2233.
- [17] a) T. Mistri, M. Dolai, D. Chakraborty, A. R. Khuda-Bukhsh, K. K. Das, M. Ali, *Org. Biomol. Chem.* **2012**, *10*, 2380–2384; b) T. Mistri, R. Alam, M. Dolai, S. K. Mandal, A. R. Khuda-Bukhsh, M. Ali, *Org. Biomol. Chem.* **2013**, *11*, 1563–1569.
- [18] H. Zheng, Z.-H. Qian, L. Xu, F.-F. Yuan, L.-D. Lan, J.-G. Xu, *Org. Lett.* **2006**, *8*, 859–861.
- [19] X. Chen, T. Pradhan, F. Wang, J. S. Kim, J. Yoon, *Chem. Rev.* **2012**, *112*, 1910–1956.
- [20] V. Thomsen, D. Schatzlein, D. Mercurio, *Spectroscopy* **2003**, *18*, 112.
- [21] a) T. Sarkar, A. Samadder, K. Ghosh, *Org. Biomol. Chem.* **2012**, *10*, 3236–3243; b) P. Mahato, S. Saha, E. Suresh, R. D. Liddo, P. P. Parnigotto, M. T. Conconi, M. K. Kesharwani, B. Ganguly, A. Das, *Inorg. Chem.* **2012**, *51*, 1769–1777.
- [22] L. Huang, X. Wang, G. Xie, P. Xi, Z. Li, M. Xu, Y. Wu, D. Baib, *Dalton Trans.* **2010**, *39*, 7894–7896.
- [23] D. F. Perkins, L. F. Lindoy, A. McAuley, G. V. Meehan, P. Turner, *Proc. Natl. Acad. Sci. USA* **2006**, *103*, 532–537.
- [24] T. Mossman, *J. Immunol. Methods* **1983**, *65*, 55–63.

Received: June 27, 2013

Published Online: October 8, 2013